

An experimental study on the resistance and movement of short pile installed in sands under horizontal pullout load

Oh Kyun Kwon¹, Jin-Bok Kim¹ and Hyuck-Min Kweon²

¹*Department of Civil Engineering, Keimyung University, Daegu, Korea*

²*Department of Railway Construction Environmental Engineering, Gyeongju University, Korea*

ABSTRACT: *In this study, the model tests were conducted on the short piles installed in sands under a horizontal pullout load to investigate their behavior characteristics. From the horizontal loading tests where dimensions of the pile diameter and length, and loading point were varied, the horizontal pullout resistance and the rotational and translational movement pattern of the pile were investigated. As a result, the horizontal pullout resistance of the pile embedded in sands was dependent on the pile length, diameter, loading point, etc. The ultimate horizontal pullout load tended to increase as the loading point (h/L) moved to the bottom from the top of the pile, regardless of the ratio between the pile length and diameter (L/D), reached the maximum value at the point of $h/L = 0.75$, and decreased afterwards. When the horizontal pullout load acted on the upper part above the middle of the pile, the pile rotated clockwise and moved to the pullout direction, and the pivot point of the pile was located at 150-360mm depth below the ground surface. On the other hand, when the horizontal pullout load acted on the lower part of the pile, the pile rotated counterclockwise and travelled horizontally, and the rotational angle was very small.*

KEY WORDS: Short pile; Horizontal loading test; Horizontal pullout resistance; Rotational angle; Loading point.

INTRODUCTION

For the construction of coastal harbor structures, there is a need to build offshore structures on the sea, unlike in the land. The foundation works of an offshore structure entails a considerable construction cost, the workability drops to a significantly low level, and in particular, the foundation works at the deep waters is a very difficult task. If the foundations of that structure are replaced with the suction piles, it will be advantageous as they can greatly save the construction costs and shorten the construction period, and make the construction works at the deep sea easier. The offshore structures built by the conventional construction method are very difficult to demolish once their construction has been completed. However, the structures which constructed with suction piles can be rapidly demolished or reconstructed if faults are found or if it is necessary to demolish them.

Suction piles, one of the foundation types used for offshore structures, can support the structure under or above the water by connecting mooring lines up to the suction pile. Up to date, there are a few studies on the bearing capacity of the suction pile considering the dimension, pullout angle, and loading point, etc. There have been several studies on the maximum resistance of the suction pile under the horizontal load with respect to different loading points, but little studies have been conducted on the movement patterns of the suction pile under the horizontal load.

Corresponding author: Oh Kyun Kwon, e-mail: ohkwon@kmu.ac.kr

This is an Open-Access article distributed under the terms of the Creative Commons Attribution Non-Commercial License (<http://creativecommons.org/licenses/by-nc/3.0>) which permits unrestricted non-commercial use, distribution, and reproduction in any medium, provided the original work is properly cited.

Therefore, the laboratory model tests on the short piles to simulate the suction piles were conducted in this study, to investigate the behavior characteristics of the suction pile. After embedding a short pile with a very small ratio of the pile length/diameter into sands under the water, then the horizontal load test was conducted. From the results of model tests, the horizontal pullout resistance of the short pile was evaluated and the characteristic of lateral movements was also investigated.

THEORETICAL CONSIDERATIONS

The conventional studies on estimating the horizontal pullout resistance of the pile embedded in sands have been conducted by Raes (1936), Broms (1964), Petrasovits and Award (1972), Meyerhof (1995), Prasad and Chari (1999), etc., and the bearing capacity of the suction pile was studied by Cho (2000), Bang and Cho (2002), Cho and Bang (2002), Kim and Jang (2011), etc. The Broms method is generally referred to as a representative method for calculating the lateral resistance of the pile in practice. Broms (1964) assumed the distributions of the deformation modes, soil reactions, and bending moments of a short pile under the horizontal load in sands, as shown in Fig. 1, where K_p is the coefficient of Rankine's passive earth pressure, and suggested a method to estimate the ultimate lateral resistance, as shown in Fig. 2. Hong (1983) proposed a method to calculate the ultimate lateral resistance by a theoretical analysis considering the failure modes between the pile and the ground.

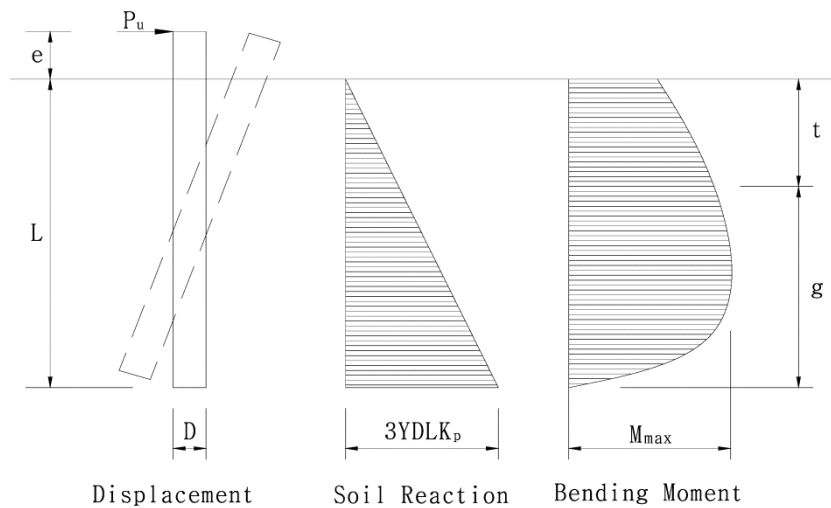


Fig. 1 Rotational and translational movements and corresponding ultimate soil resistance for the free headed short piles in sands under lateral loads (Broms, 1964).

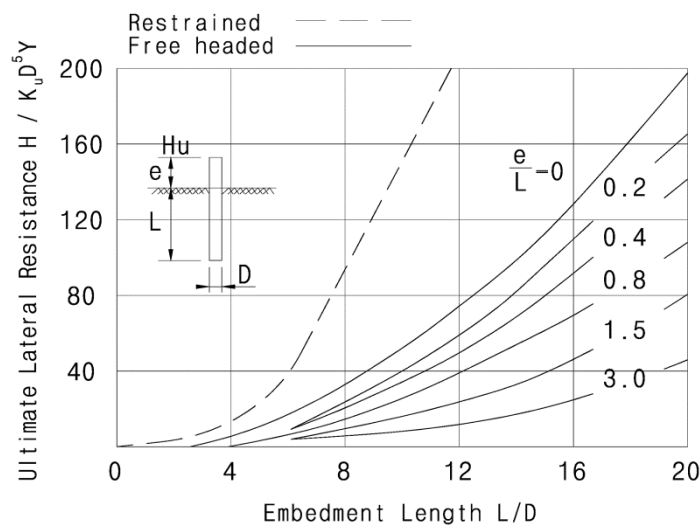


Fig. 2 Broms's solution for ultimate lateral resistance of the short piles in sands (Broms, 1964).

Bang and Cho (2002) reported that the pullout resistance of the suction anchor was affected by various factors, such as the soil type, loading direction, loading point, embedment depth, and anchor size etc. They reported, as the results of the study on the suction anchor under the lateral load, that the maximum lateral resistance occurred when the lateral load was acted at a depth of $0.8L$ of the pile, and that the lateral resistance increased as the length of the pile increased. Cho (2000) reported from an analytical study that the maximum ultimate lateral resistance of the suction pile embedded in sands occurred at a depth of $0.8L$ from the top of the pile, as shown in Fig. 3. Kim and Jang (2011) conducted the centrifuge model tests on the suction pile under pullout loading according to the inclination angle, and reported that the maximum lateral resistance of the suction pile occurred when the lateral loading point was acted at a depth of around $0.75L$ from the top of the pile (see Fig. 4).

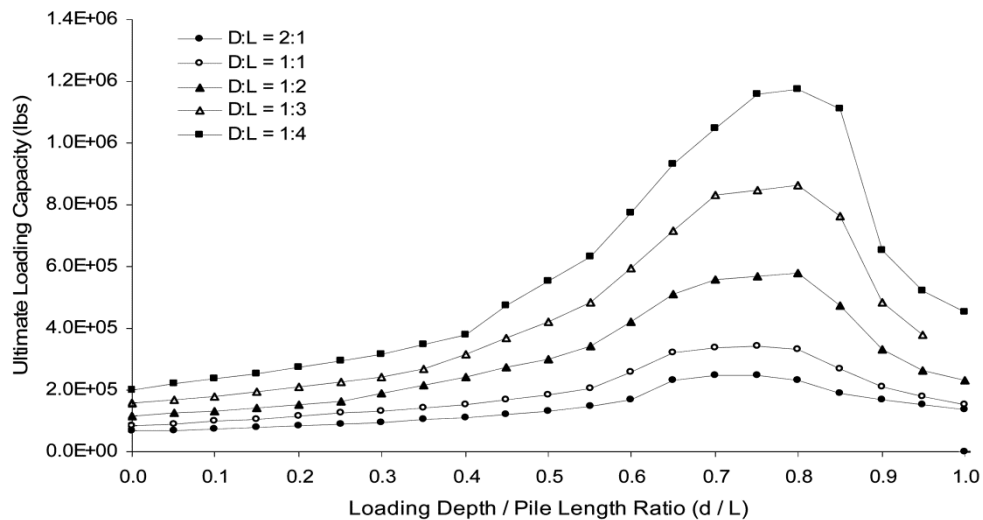


Fig. 3 Ultimate lateral resistance of the suction pile in sands (Cho, 2000).

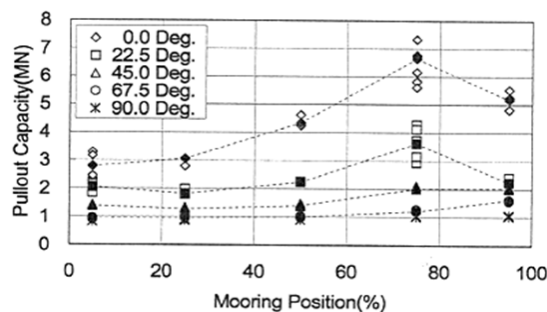


Fig. 4 Relationship between pullout capacity and mooring position (Kim and Jang, 2011).

MODEL TEST APPARATUS AND PROCEDURES

In this study, the laboratory model tests were conducted to investigate the pullout behavior characteristics of the suction pile which was embedded in sands under the water. The model soil chamber was manufactured using steel materials and acrylic to prevent the frame from being deformed by the loading. The size of the model apparatus was $1,280mm \times 1,000mm \times 1,500mm$ (width \times length \times height), and its cross-sectional diagram is shown in Fig. 5 (see Fig. 6). As shown in this figure, the loading system was designed using pulleys, and the model tests were executed by loading the horizontal pullout loads on the short pile embedded in sands under the water. A partition wall was installed on the right-hand side of the model soil chamber, and there was a gap about $5mm$ wide in the partition wall. The pullout load was applied with the wire connected to the model pile through this gap. To prevent the soil particles from leaking through this gap, a thin non-woven fabric was attached onto the area around the gap (Kim, 2009).

The Jumunjin standard sands were used in the model test. The grain size distribution curve of the sands as shown in Fig. 7 was classified as SP according to the Unified Soil Classification System (USCS), with a uniformity coefficient (C_u) of 1.38, a

coefficient of curvature (C_c) of 0.97, and specific gravity (G_s) of 2.62. The relative density of the sands was determined by measuring the unit weight using the cans installed in the sand layer. The minimum dry unit weight (γ_{dmin}) of the sands was measured by falling the sand particles free in the water, and the maximum dry unit weight (γ_{dmax}) was measured by the Bowles method (Bowles, 1978). The minimum and maximum dry unit weight was 13.43 and 16.37 kN/m^3 respectively. The relative density of the model sands was approximately 65%, and the internal friction angle was measured at about 35 degrees (Kim, 2009).

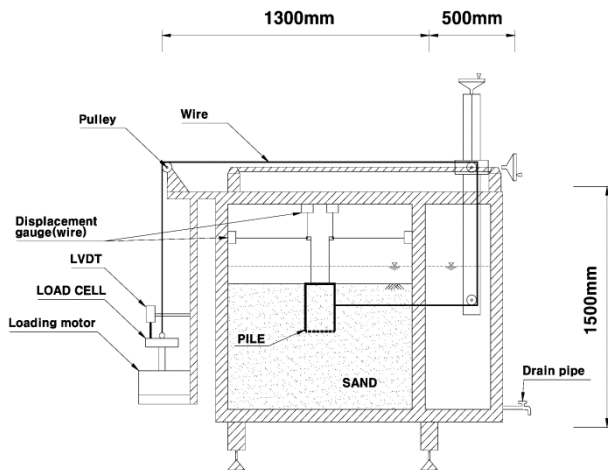


Fig. 5 Schematic diagram of the model apparatus.



Fig. 6 Picture of the model chamber.

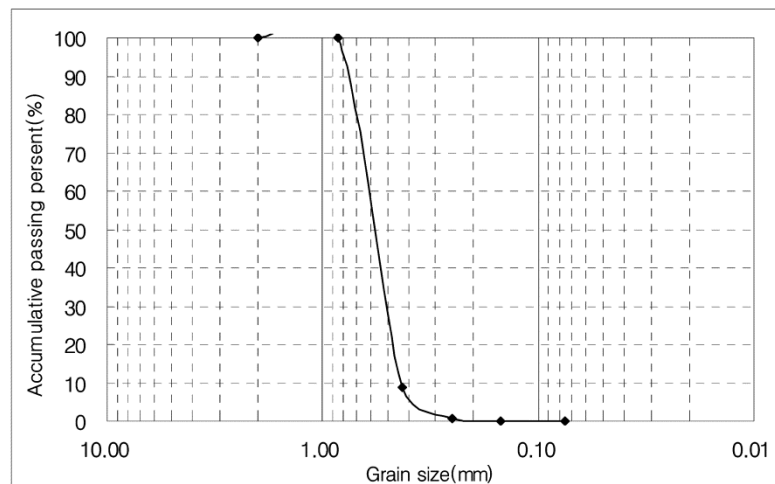


Fig. 7 Grain size distribution curve of sands used in the test.

The piles used in the model test were made of the acrylic with three different diameters ($D = 100, 150, \text{ and } 200\text{mm}$), two different length/diameter ratios ($L/D = 1 \text{ and } 2$), and 5mm thickness. They were assumed as perfectly rigid. Five 3mm -diameter holes are drilled on the side of the model pile, and are connected by the wire to load the horizontal pullout. There are 5 loading points in side of the pile, which are $0.05L, 0.25L, 0.5L, 0.75L, \text{ and } 0.95L$ apart from top of the pile.

The procedures of model test were as followed. First, the sand layer was built up in the model chamber by pouring the sand particles under the water. The model pile was embedded to the desired location, and then the model pile was connected to the pullout loading system with the wire. And four wire displacement transducers were separately connected at two positions of the pile top, in the vertical and horizontal directions respectively. The horizontal and vertical displacements of the pile were measured during loading the pullout to investigate the moving behavior of the pile. As the pile moved in the vertical and horizontal directions and simultaneously rotated during the horizontal load test, at least the coordinates at two points of the pile should be measured to investigate the exact moving path of the pile. For such purpose, in this study, two steel bars were connected to the top of the model pile to measure the coordinates at two points, and the exact moving path of the model pile was investigated

using the measured coordinates. The pullout load was applied at a speed of $2\text{mm}/\text{min}$., and was measured by the load cell (with a capacity of 19.6 kN). The loads and displacements of the model pile were acquired by a data logger (TDS-602) during the horizontal loading test (Kim, 2009).

MODEL TEST RESULTS AND DISCUSSION

In this study, the model tests were executed to investigate the behavior characteristics of the suction pile embedded in sands under the horizontal pullout load. The short pile with a small ratio of L/D to simulate the suction pile was used in the model tests, and the horizontal loading test was executed with varying the diameter and length of the pile, and loading point. The pile with a diameter of 200mm and length of 400mm was excluded from the model tests in this study due to the size of the test soil chamber and the pile materials.

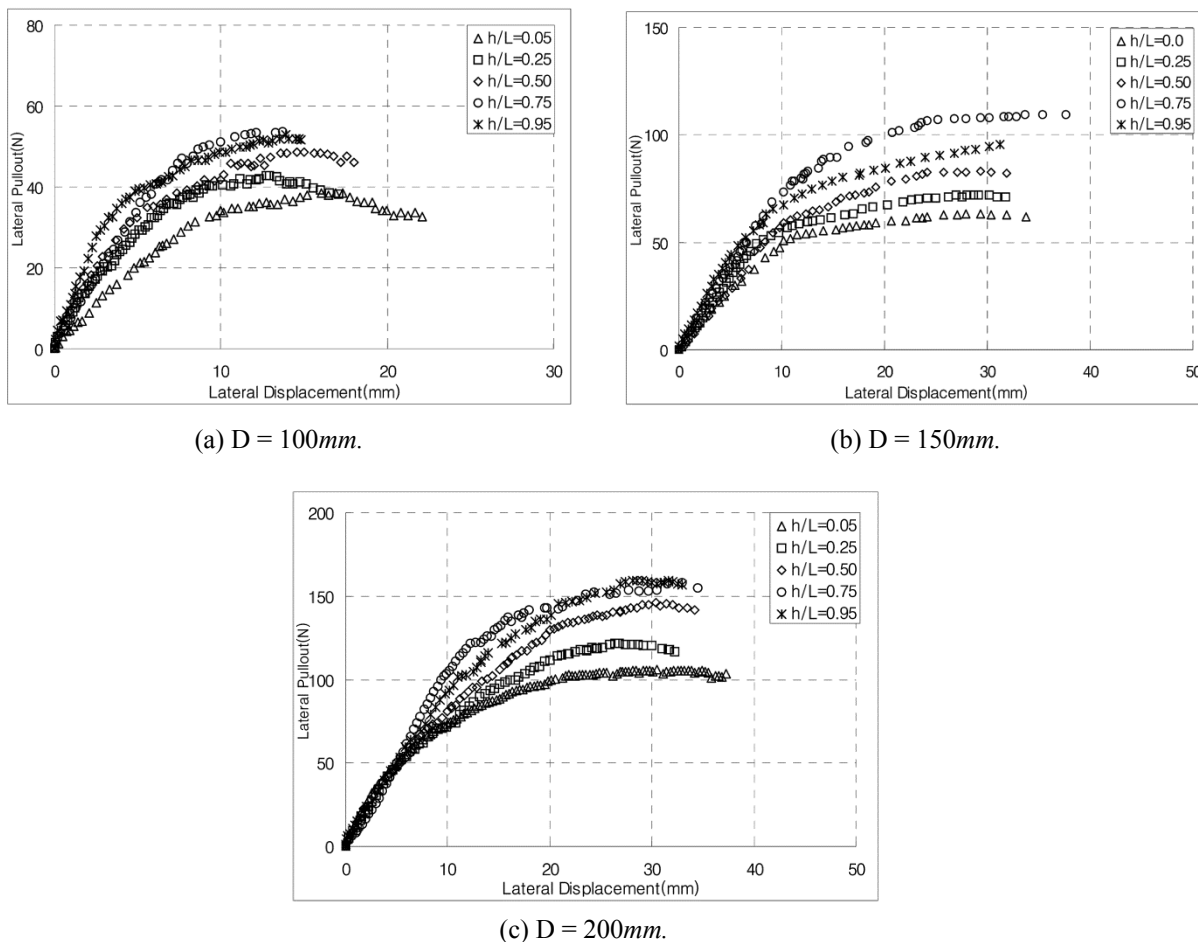


Fig. 8 Relationship between the horizontal pullout load and displacement of the pile with $L/D = 1$.

Figs. 8 and 9 show the horizontal pullout load vs. displacement curves in various cases from the model test. Fig. 8 presents the case with the ratio of L/D of 1, and Fig. 9 the case with the ratio of L/D of 2. These figures show the relationships between the horizontal pullout load and displacement at the different loading points. As a result of model tests, the ultimate horizontal pullout load increased in all cases, regardless of the pile length and diameter, as the loading point moved down to the bottom of the pile from the top, then the maximum value was occurred at approximately $h/L = 0.75$, and decreased afterwards. Such results coincided with the results of the centrifuge model tests conducted by Kim and Jang (2011), and appeared similar to the results of Cho (2000). And as the pile diameter and length increased, the ultimate horizontal pullout load increased, and the initial slope of the horizontal pullout load vs. displacement curve also increased slightly. Table 1 presents the ultimate horizontal pullout load evaluated from the horizontal pullout load vs. displacement curves by the model tests. In this study, the ultimate

horizontal pullout load was evaluated using three methods: the maximum load method, Davisson (1972) method, and $\Delta = 0.1 D$ method (Terzaghi, 1943), and the average values of the ultimate horizontal pullout loads evaluated using those methods are presented in Table 1. Fig. 10 shows the relationship between the loading point and the horizontal pullout load, where the dotted line represents the case of $L/D = 1$ and the solid line the case of $L/D = 2$. As shown in Fig. 10, all the cases show a tendency for the ultimate horizontal pullout load to increase as the loading point moves down to the bottom of the pile, regardless of the length and diameter of pile, to present the maximum value at approximately $h/L = 0.75$, and to decrease afterwards. In addition, the ultimate horizontal pullout load increased as the length and diameter of the pile increased.

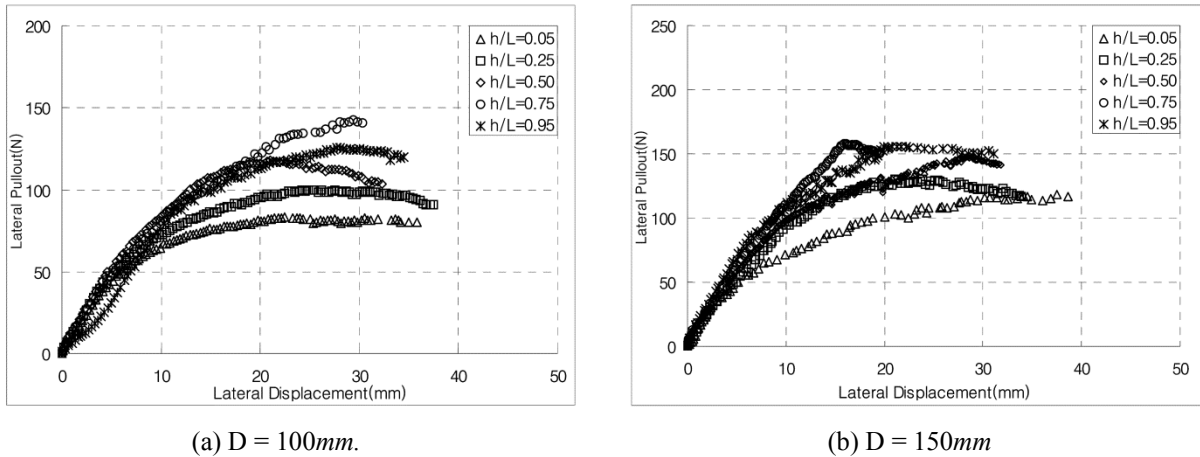


Fig. 9 Relationship between the horizontal pullout load and displacement of the pile with $L/D = 2$.

Table 1 Ultimate horizontal pullout load (P_{ult}) from the model tests. (unit: N)

P_{ult}		h/L	0.05	0.25	0.50	0.75	0.95
$L/D = 1$	$D = 100mm$		34.9	41.3	45.4	52.7	50.3
	$D = 150mm$		57.9	64.6	73.1	98.3	83.9
	$D = 200mm$		100.2	115.3	130.4	150.3	144.0
$L/D = 2$	$D = 100mm$		75.0	87.9	105.0	124.0	113.1
	$D = 150mm$		101.6	125.4	137.8	154.0	146.2

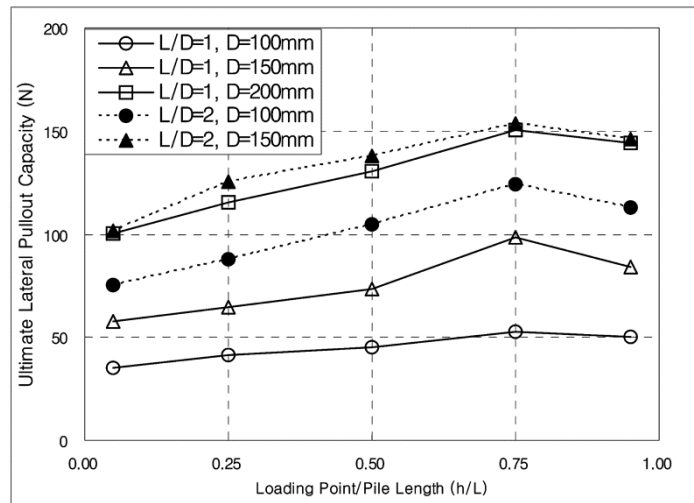
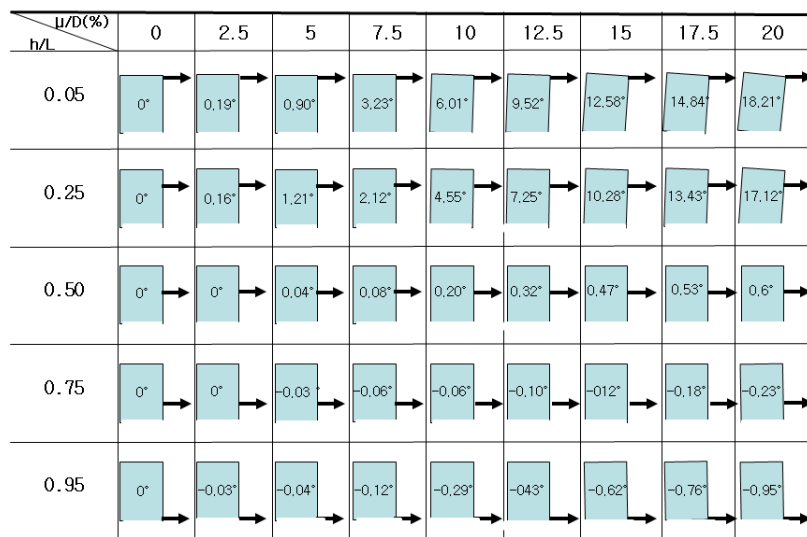
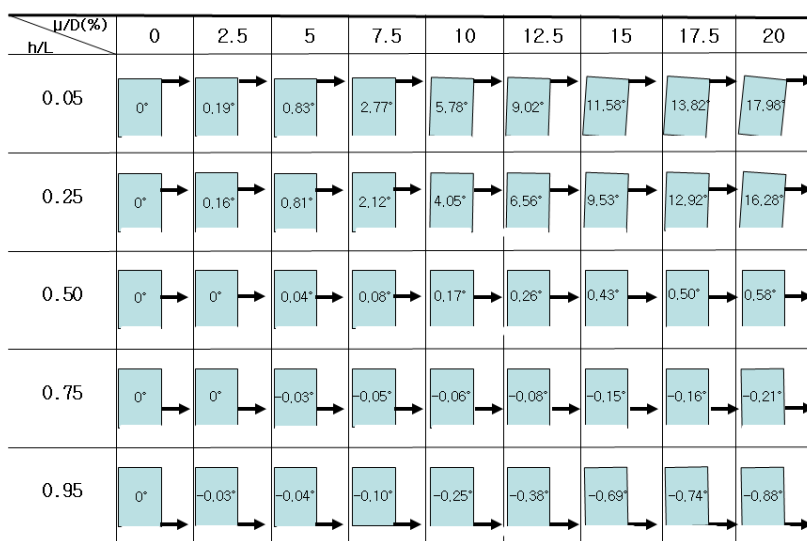


Fig. 10 Relationship between the ultimate pullout load and the loading point.

In this study, to investigate the movement pattern of the pile during loading the horizontal pullout precisely, the wire displacement transducers were separately connected to the two points at the top of the model pile in the horizontal and vertical directions, and the coordinates at the two points were measured. When the horizontal pullout load applied to the pile, the pile moved towards the pullout direction and rotated simultaneously. Fig. 11 shows the rotational and translational movements of the pile during loading the horizontal pullout, which are the result of the model test on the pile with a diameter of 150mm. Fig. 11(a) shows the test results of the case of $L/D = 1$, and (b) the case of $L/D = 2$. From these figures, when the horizontal pullout load acted at the upper part above the middle of the pile, the upper part of the pile rotated clockwise and moved to the pullout direction, i.e. experienced rotational and translational movements simultaneously. And as the loading point was moved to the lower part of the pile from the top, the rotational angle of the pile decreased. On the other hand, when the horizontal pullout load acted at the lower part of the pile, the upper part of the pile moved horizontally with rotating counterclockwise (i.e., the opposite direction of the pullout loading), but the rotational angle of the pile was very small. Table 2 presents the rotational angles of the pile when a horizontal displacement corresponds to 10% of the pile diameter. As the loading point moved down from the top of the pile to the bottom, the rotational angle of the pile decreased, and the pile showed a tendency to move horizontally almost without rotating at $h/L = 0.5$ and 0.75 . In addition, as the ratio of L/D increased, the rotational angle decreased.



(a) case of $L/D = 1$.



(b) case of $L/D = 2$.

Fig. 11 Rotational movement patterns of the pile with a diameter of 150mm under the horizontal pullout load.

Table 2 Rotational angles at the displacement corresponding to 10% of the pile diameter.

	L/D = 1			L/D = 2	
	D = 100mm	D = 150mm	D = 200mm	D = 100mm	D = 150mm
h/L = 0.05	5.01°	6.01°	7.04°	2.08°	5.78°
h/L = 0.25	3.40°	4.55°	9.82°	1.22°	4.05°
h/L = 0.50	0.28°	0.20°	0.31°	0.10°	0.17°
h/L = 0.75	-0.82°	-0.60°	-0.03°	-0.07°	-0.06°
h/L = 0.95	-1.23°	-0.29°	-0.34°	-0.13°	-0.25°

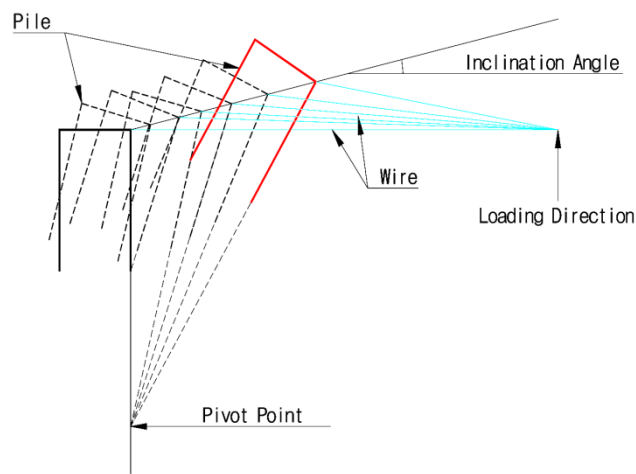


Fig. 12 Schematic diagram of the rotation and movement pattern of the pile under the horizontal pullout load.

When the horizontal pullout load acted at the side surface of the pile, the pile generally moved to the pullout direction and rotated simultaneously. As explained earlier, the movement patterns of the pile are varied depending on the loading position where the pullout load acts. Fig. 12 shows the translational and rotational movement pattern of the pile in the case of loading on the top end ($h/L = 0.05$) of the pile. As shown in Fig. 12, the pile under the horizontal pullout load appeared to have been moving while rotating around a certain pivot point. Such tendency was similarly observed at all the piles that were used for the model test. The pivot point of the pile under the horizontal pullout load can be calculated using the coordinate values at the two points measured during the horizontal loading test. The movement path of the pivot points calculated with such method is presented in Fig. 13, which is the case of a pile of 150mm diameter with the ratio of L/D of 1. When the horizontal pullout load acted at the upper part of the pile, the pile rotated clockwise and moved the pullout direction, and the pivot point of the pile was located at about 200-220mm (i.e., $1.33L \sim 1.47L$) depth below the ground surface. When the horizontal pullout load acted at the middle of the pile, the pile initially moved horizontally, then continued moving and rotating repeatedly, and the pivot point of the pile was located irregularly at about 250-350mm (i.e., $1.67L \sim 2.33L$) depth below the ground surface. On the other hand, when the horizontal pullout load acted at the lower part of the pile, the pile moved almost horizontally, and the pivot point of the pile was located at approximately -20~-25mm (i.e., $-0.13L \sim -0.17L$) below the ground surface.

Table 3 presents the position of the pivot point of the pile under the horizontal pullout load according to the diameter and length of the pile, and the loading point. When the horizontal pullout load acted at the upper part above the middle of the pile, the pivot point of the pile was positioned at 150-360mm (i.e., $1.0L \sim 2.4L$) depth below the ground surface. On the other hand, when the horizontal pullout load acted at the lower part of the pile, the pivot point of the pile was positioned at 20-100mm (i.e., $0.13L \sim 0.67L$) depth below the ground surface, except the pile of 100mm diameter with $L/D = 1$. As a result, the pivot point of the pile moved closer to the ground surface as the loading point moved down to the lower part of the pile, while the pivot point moved to the deeper depth below the ground surface as the ratio of L/D increased.

From Fig. 13 and Table 3, the pivot point of the pile was positioned below the ground when the horizontal pullout load acted at the upper part above the middle of the pile, while the pivot point moved close to the ground surface when the load acted at the lower part of the pile. This means that the translational and rotational movements of the pile under the pullout load were irregularly occurred at the initial stage, but when the load increased to some extent, the pile rotated and moved around a certain pivot point. That is, when the horizontal pullout load acts at the pile, the pile doesn't rotate from the beginning. The pile is located to a certain position in the soils as the other part of the pile not to be acted the pullout load moves slightly towards the opposite direction to the pullout direction, then the pile moves to the pullout direction. And afterwards, the pile rotates and moves around a pivot point.

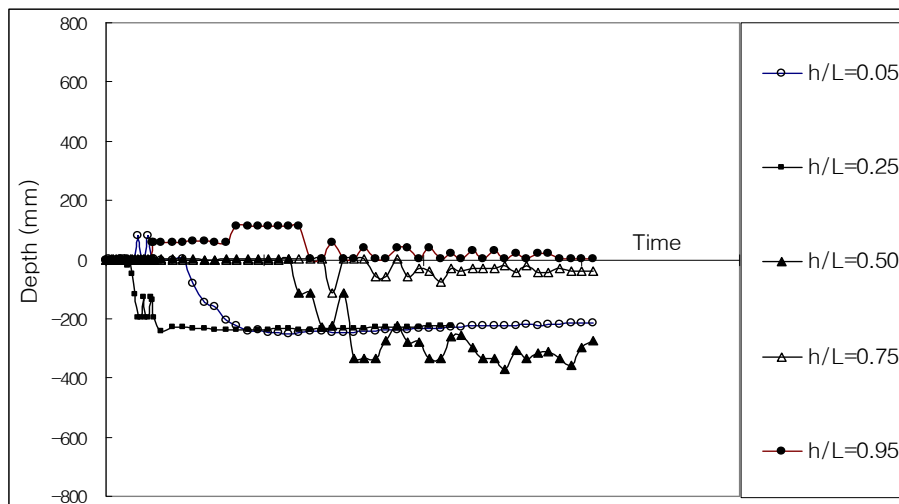


Fig. 13 Movement path of the pivot point according to the time in the case of the pile with $L/D = 1$ and $D = 150mm$.

Table 3 Depth of the pivot point under the horizontal pullout load.

(unit: mm)

	L/D = 1			L/D = 2	
	D = 100	D = 150	D = 200	D = 100	D = 150
$h/L = 0.05$	-230	-200	-150	-300	-200
$h/L = 0.25$	-230	-220	-250	-300	-235
$h/L = 0.50$	-230~-300	-250~-350	-280~-360	-280~-360	-200
$h/L = 0.75$	-20	-25	-50	-80	-100
$h/L = 0.95$	-20	20	-25	-25	-50

The pile under the horizontal pullout load rotates and moves horizontally, and the loading points always vary non-parallel to the ground surface during loading the pullout. The position of loading point can be calculated from the coordinates at two points of the pile under the horizontal pullout load. Fig. 14 shows the movement path of the loading points calculated from the results of the horizontal load test on the pile of 150mm diameter with $L/D = 1$. The loading point moved to the horizon with being tilted about 26 degrees in the case when the horizontal pullout load acted on the top of the pile ($h/L = 0.05$), about 24° in the case of $h/L = 0.25$, 16.7° in the case of $h/L = 0.5$, 12.7° in the case of $h/L=0.75$, and almost parallel to the ground surface in the case of $h/L = 0.95$. From these results, the pile under the horizontal pullout load moved towards the pullout direction with being pulled out upwards. As the loading point moved up to the upper of the pile from the bottom, the pullout displacement of pile increased. The model test results on the inclination angle of the path along which the loading point moves are presented in

Table 4. From this table, when the horizontal pullout load acts at the bottom of the pile, the movement path of the loading point pile moves horizontally almost without being inclined. In addition, all the cases showed a tendency for the inclination angle of the loading point path to decrease as the loading point moved down from the top of the pile to the bottom and the ratio of L/D increased.

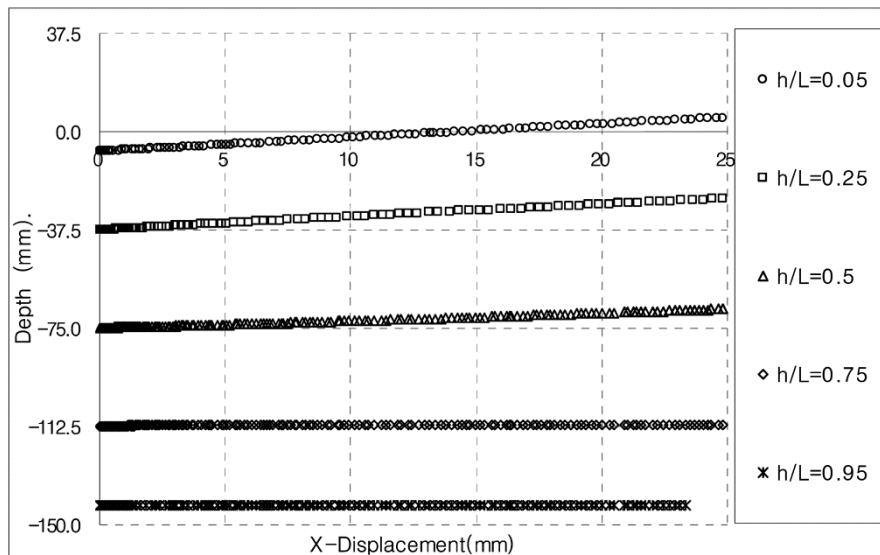


Fig. 14 Movement path of loading point of the pile of 150mm diameter with $L/D = 1$.

Table 4 Inclination angle of movement path of the loading point under the horizontal pullout load.

	$L/D = 1$			$L/D = 2$	
	$D = 100mm$	$D = 150mm$	$D = 200mm$	$D = 100mm$	$D = 150mm$
$h/L = 0.05$	34°	26.16°	23°	22.8°	16°
$h/L = 0.25$	30.5°	25.05°	18°	17.2°	9.6°
$h/L = 0.50$	23.9°	17.07°	13.5°	11.8°	5°
$h/L = 0.75$	1.58°	1.27°	0.82°	0.85°	0.15°
$h/L = 0.95$	0.97°	0.06°	0.05°	0.03°	0.07°

CONCLUSIONS

The lateral behavior characteristics of the suction pile installed in sands was investigated in this study. The laboratory model tests were conducted on the pile with small ratio of L/D , to simulate the suction pile. From the tests which were varied the diameter and length of the pile and loading points, the horizontal pullout load and the translational and rotational movements of the pile were investigated, and the following conclusions were obtained.

As a result of model tests, the ultimate horizontal pullout load of the pile embedded in sands increased as the loading point (h/L) moved down to the bottom from the top of the pile, regardless of the ratio of L/D , presented the maximum value at $h/L = 0.75$, and decreased afterwards. When the horizontal pullout load acted on the upper part above the middle of the pile, the pile rotated clockwise and moved to the pullout direction, and the pivot point of the pile was positioned at $150\text{--}360mm$ (i.e., $1.0L\text{--}2.4L$) depth below the ground surface. On the other hand, when the horizontal pullout load acted on the lower part of the pile, the pile rotated counterclockwise and moved to the pullout direction, and the rotational angle was very small. The pivot point of the pile was positioned at $20\text{--}100mm$ depth (i.e., $0.13L\text{--}0.67L$) below the ground surface. Thus, the inclination angles of the

loading point path showed a tendency to decrease in all cases as the loading point of the horizontal pullout load moved down to the bottom of the pile from the top, and as the ratio of L/D increased. In addition, the rotational angle of the pile became smaller, and the pivot point of the pile appeared moving closer to the surface of the earth.

ACKNOWLEDGEMENT

This study was financially supported by Korea Institute of Construction & Transportation Technology Evaluation and Planning Grant No. B04-01 and Korea Institute of Energy Technology Evaluation and Planning Grant No. 20103020070080 funded by the South Korean government (MOCT and MOTIE, respectively). This study was conducted with the support of the regional characterization research and development project (the next-generation coastal-space acquisition technology) of the Ministry of Land, Transport, and Maritime Affairs and the new/renewable energy fusion source technology development project of the Ministry of Commerce, Industry, and Energy of South Korea. This material is based on work supported by Korea Institute of Energy Technology Evaluation and Planning under Grant No. 20103020070080.

REFERENCES

- Bang, S. and Cho, Y., 2002. Ultimate horizontal loading capacity of suction pile. *International Journal of Offshore and Polar Engineering*, 12(1), pp.56-63.
- Bowels, J.E., 1978. *Engineering properties of soils and their measurements*. 2nd ed. New York: McGraw-Hill.
- Broms, B.B., 1964. The lateral resistance of piles in cohesionless soils. *Journal of Soil Mechanics and Foundation Division, American Society of Civil Engineers*, 90(3), pp.123-156.
- Cho, Y.K., 2000. *Calibration of installation, analytical performance study, and analytical solution of loading capacity of suction piles*. Ph.D. South Dakota School of Mines and Technology.
- Cho, Y. and Bang, S., 2002. Inclined loading capacity of suction piles. *Proceedings of 12th International Offshore and Polar Engineering Conference*, Kitakyushu, Japan, 26-31 May 2002, 2, pp.827-832.
- Davisson, M., 1972. High capacity piles. *Proceedings of Lecture Series on Innovations in Foundation Construction, American Society of Civil Engineers, Illinois Section, Chicago, IL*, pp.81~112.
- Hong, W.P., 1983. Piles Subjected to Lateral Loads. *Korean Society of Civil Engineers*, 31(5), pp.32-36.
- Kim, J.B., 2009. *A Study on behavior characteristics of suction pile subjected to oblique pull in sands*. Ph.D. Keimyung University.
- Kim, Y.S. and Jang, Y.S., 2011. Analysis of load capacity and deformation behavior of suction pile installed in sand. *Journal of The Korean Geotechnical Society*, 27(11), pp.27-37.
- Meyerhof, G.G., 1995. Behavior of pile foundations under special loading conditions: 1994 R.M. Hardy Keynote Address. *Canadian Geotechnical Journals*, 32(2), pp.204-222.
- Petrasovits, G. and Awad, A., 1972. Ultimate lateral resistance of a rigid pile in cohesionless soil. *Proceeding of The 5th European Conference on Soil Mechanics and Foundation Engineering*, Madrid, 10-13 April 1972, 1, pp.407-412.
- Prasad, Y.V.S. and Chari, T.R., 1999. Lateral capacity of model rigid piles in cohesionless soils. *Soils and Foundations*, 39(2), pp.21-29.
- Raes, P.E., 1936. Theory of lateral bearing capacity of piles. *Proceeding of The 1st International Conference on Soil Mechanics and Foundation Engineering*, Massachusetts, USA, 22-26 June 1936, pp.166-169.
- Terzaghi, K., 1943. *Theoretical soil mechanics*. New York: John Wiley and Sons.